

# Lung dose measured on post-radioembolization $^{90}\text{Y}$ -PET/CT and incidence of radiation pneumonitis

*Short running title:*  $^{90}\text{Y}$ -SIRT lung dose and lung toxicity

Martina Stella\*, Rob van Rooij, Marnix GEH Lam, Hugo WAM de Jong and Arthur JAT Braat

\*Corresponding author

Affiliation of all authors: Division of Imaging and Oncology, University Medical Center Utrecht, Utrecht  
University

Corresponding author:

Martina Stella, MSc

ORCID ID: 0000-0001-9794-3184

+31887556295

[M.Stella@umcutrecht.nl](mailto:M.Stella@umcutrecht.nl)

University Medical Center Utrecht

Heidelberglaan 100

3584 CX Utrecht, NL

## ABSTRACT

Radiation pneumonitis is a rare but possibly fatal side effect of Yttrium-90 ( $^{90}\text{Y}$ ) radioembolization. It may occur 1 to 6 months after therapy, in case a significant part of the  $^{90}\text{Y}$  microspheres shunt to the lungs. In current clinical practice, a predicted value of lung dose greater than 30Gy is considered a criterion to exclude patients from treatment. However, contrasting findings regarding the occurrence of radiation pneumonitis and lung dose were previously reported in literature. In this study, the relationship between the lung dose value and the eventual occurrence of radiation pneumonitis after  $^{90}\text{Y}$  radioembolization was investigated.

**Methods:** A total of 317  $^{90}\text{Y}$  liver radioembolization procedures performed during an 8-years period (Feb.2012–Sep.2020) were retrospectively analyzed. Predicted lung mean dose using  $^{99\text{m}}\text{Tc}$ -MAA planar scintigraphy ( $\text{LMD}_{\text{MAA}}$ ) acquired during the planning phase and left lung mean dose ( $\text{LMD}_{\text{Y-90}}$ ) using the  $^{90}\text{Y}$  PET/CT acquired after the treatment were calculated. For the lung dose computation, it was chosen to use the left lung as representative lung volume, to compensate for the scatter from the liver moving in the cranial-caudal direction due to breathing and mainly affecting the right lung. **Results:** Two hundred and seventy-two patients underwent  $^{90}\text{Y}$  procedures, of which 63% performed with glass microspheres and 37% with resin microspheres. Median injected activity was 1974MBq (range: 242-9538MBq). Median  $\text{LMD}_{\text{MAA}}$  was 3.5Gy (range: 0.2–89.0Gy). For 14 procedures  $\text{LMD}_{\text{MAA}}$  was >30Gy. Median  $\text{LMD}_{\text{Y-90}}$  was 1Gy (range: 0.0–22.1Gy). No patients had a  $\text{LMD}_{\text{Y-90}}$  >30Gy. Of the three patients with a  $\text{LMD}_{\text{Y-90}}$  >12Gy, two patients ( $\text{LMD}_{\text{Y-90}} = 22.1\text{Gy}$ ,  $\text{LMD}_{\text{MAA}} = 89\text{Gy}$  and  $\text{LMD}_{\text{Y-90}} = 17.7\text{Gy}$ ,  $\text{LMD}_{\text{MAA}} = 34.1\text{Gy}$ , respectively) developed radiation pneumonitis and consequently died. A third patient with a  $\text{LMD}_{\text{Y-90}}$  equal to 18.4Gy ( $\text{LMD}_{\text{MAA}} = 29.1\text{Gy}$ ) died 2 months after treatment, before imaging evaluation, due to progressive disease. **Conclusion:** The occurrence of radiation pneumonitis as a consequence of lung shunt following  $^{90}\text{Y}$  radioembolization is rare (<1 %). No radiation pneumonitis developed in cases with a measured  $\text{LMD}_{\text{Y-90}}$  lower than 12Gy.

**Key words:**  $^{90}\text{Y}$  radioembolization; lung-dose; radiation pneumonitis;  $^{90}\text{Y}$  PET dosimetry;  $^{99\text{m}}\text{Tc}$ -MAA lung dose predicted

## INTRODUCTION

Radioembolization is a well-established treatment for primary and metastatic liver malignancies<sup>1</sup>. It is defined as the injection via percutaneous trans-arterial techniques<sup>2</sup> of embolic particles (diameter size range: 20 – 60µm) loaded with yttrium-90 (<sup>90</sup>Y) or holmium-166 (<sup>166</sup>Ho). As hepatic tumors are preferentially fed by the blood supply from the hepatic artery, radioembolization preferentially deposits radioactive microspheres in the peritumoral and intratumoral arterial vasculature through the hepatic artery, relatively sparing normal liver parenchyma<sup>3</sup>. Three devices are commercially available: glass <sup>90</sup>Y microspheres (TheraSphere®; Boston Scientific Corporation, Marlborough, Massachusetts, US), resin <sup>90</sup>Y microspheres (SIR-spheres®; SIRTex Medical Limited, North Sydney, NSW, Australia) and poly-L-lactic acid <sup>166</sup>Ho microspheres (QuiremSpheres®; Quirem BV, Deventer, The Netherlands). Since microspheres can pass through tumor-associated arteriovenous shunts and lodge in the pulmonary vasculature, if this pulmonary deposition is significant, a dose-dependent radiation-induced pneumonitis may ensue. Therefore, presence of significant hepatopulmonary shunting is a relative contraindication for radioembolization. The current approach to radioembolization with respect to radiation pneumonitis is mainly driven by two seminal publications<sup>4,5</sup> that have strongly influenced the guidance on lung dose limits following radioembolization. Based on clinical evidence from these studies, lung dose limit of 30Gy was recommended for single radioembolization treatment<sup>6</sup> and adopted in the instructions for use manual (IFU) of these devices. For this reason, the assessment of the lung shunt fraction (LSF), which is a prediction of the eventual lung dose following the radioembolization treatment, is paramount prior to the administration of the radioactive particles.

For <sup>90</sup>Y, this prediction is performed using <sup>99m</sup>Tc-macroaggregated albumin (<sup>99m</sup>Tc-MAA). Despite being the current clinical practice, <sup>99m</sup>Tc-MAA is poor in predicting the dose to the lungs, especially when computing the lung shunt fraction (LSF<sub>MAA</sub>), and consequently the predicted lung mean dose (LMD<sub>MAA</sub>) using planar scintigraphy. SPECT/CT imaging technique can improve the LSF computation<sup>7</sup>. However, discrepancies between <sup>90</sup>Y and <sup>99m</sup>Tc-MAA particles reduce its predictive value<sup>8,9</sup>.

The aim of this study is to assess the occurrence of radiation pneumonitis after  $^{90}\text{Y}$  liver radioembolization and perform lung dosimetry on  $^{90}\text{Y}$ -PET/CT to evaluate the currently assumed lung dose restriction of  $<30\text{Gy}$ . Although multiple studies on lung dose following  $^{90}\text{Y}$  radioembolization are reported in literature, they all focus on the  $^{99\text{m}}\text{Tc}$ -MAA based lung dose estimate during the pre-treatment phase. Conversely, this study retrospectively quantified the actual dose received by the lungs following  $^{90}\text{Y}$  radioembolization, exploiting the potential of post-treatment PET/CT<sup>10</sup> and  $^{90}\text{Y}$  accurate dosimetry<sup>11</sup>. This would provide a better insight into the lung dose following  $^{90}\text{Y}$  radioembolization and the related occurrence of radiation pneumonitis.

## **MATERIALS AND METHODS**

This single center, retrospective analysis of all patients treated with  $^{90}\text{Y}$ -radioembolization between February 2012 and September 2020 was approved by the ethical research committee and the need for informed consent was waived. Prior to radioembolization treatment, patient eligibility for treatment was assessed by  $^{99\text{m}}\text{Tc}$ -MAA injection in the hepatic artery, to assess intrahepatic distribution and potential extrahepatic deposition of activity (including lung shunting). After  $^{99\text{m}}\text{Tc}$ -MAA injection, a planar gamma camera scintigraphy (for  $\text{LSF}_{\text{MAA}}$  computation) and a SPECT/CT (to visually assess extrahepatic depositions) were acquired. To assess the treatment outcome, a post-treatment  $^{90}\text{Y}$ -PET/CT was obtained the same day or the day after treatment. Lung mean dose after  $^{90}\text{Y}$  radioembolization was assessed using the post-treatment  $^{90}\text{Y}$  PET/CT.

### **$^{90}\text{Y}$ -PET/CT protocol**

Images were acquired on a Biograph mCT time-of-flight PET/CT scanner or on a Biograph Vision 600 time-of-flight PET/CT scanner (both Siemens Medical Solutions USA, Inc.), with a 40- and 64-slice CT scanner, respectively. To reconstruct the images, an iterative algorithm including a model-based scatter correction method, which encompasses a point spread function model of the detector response together with time-of-flight information, was used. To correct for attenuation, low-dose CT acquired right after the PET

was employed. Both PET scanners and reconstruction protocol were validated for  $^{90}\text{Y}$  quantitative imaging<sup>12</sup>.

### **$^{99\text{m}}\text{Tc}$ -MAA based lung mean dose predicted**

To determine patient's eligibility, lung mean dose predicted using  $^{99\text{m}}\text{Tc}$ -MAA ( $\text{LMD}_{\text{MAA}}$ ) was calculated as follows:

$$\text{LMD}_{\text{MAA}} = \frac{\text{Activity}_{\text{prescribed}}[\text{GBq}] \times \text{LSF}_{\text{MAA}} \times 50[\text{Gy} \times \text{kg}/\text{GBq}]}{\text{Lung mass} [\text{kg}]}$$

Where lung mass is assumed to be equal to 1 kg and 50 [Gy\*kg/GBq] is the standard conversion factor for  $^{90}\text{Y}$ .  $\text{LSF}_{\text{MAA}}$  is the lung shunt fraction based on the  $^{99\text{m}}\text{Tc}$ -MAA planar image and was computed as follows:

$$\text{LSF}_{\text{MAA}} = \frac{\text{Count}_{\text{Lungs}}}{\text{Count}_{\text{Lungs}} + \text{Count}_{\text{Liver}}} \times 100\%$$

The counts were computed using the geometric mean following standard clinical practice<sup>13</sup>. Lungs and liver were delineated on the planar scintigraphy by the imaging technicians.

### **$^{90}\text{Y}$ PET-based lung mean dose**

To assess the mean absorbed dose in the lungs after the treatment, lungs masks were automatically segmented on the CTs corresponding to the PET scans used for the dosimetric purposes, using a freely available U-net, extracting right-left lung separately<sup>14</sup>. All masks were visually checked to ensure a correct segmentation. Since right lung was affected by scatter from the liver moving in the cranial-caudal direction due to breathing (see FIGURE.1), only the left lung was considered, as representative for the computation of the mean lung dose.  $^{90}\text{Y}$  PET based left lung mean dose ( $\text{LMD}_{\text{Y-90}}$ ) was computed as follows:

$$\text{LMD}_{\text{Y-90}} = \frac{\text{Mean Activity Concentration}_{\text{LEFT LUNG}} \left[ \frac{\text{Bq}}{\text{mL}} \right] \times 5 \times 10^{-8} [\text{J} * \text{s}]}{\text{Lung density} [\text{kg}/\text{cm}^3]}$$

Mean activity concentration in the left lung was computed as the mean of the voxel value [Bq/mL] within the left lung mask. Lung density was assumed to be  $2.6e^{-4}$  [kg/mm<sup>3</sup>]<sup>15</sup>, while  $5e^{-8}$  [J\*s] represents the deposited energy due to the  $\beta$  decay of 1 Bq of injected <sup>90</sup>Y activity<sup>16</sup>. Mean activity concentration was corrected for <sup>90</sup>Y decay considering the time difference between the activity administration time and the scanning time. Three commonly applied assumptions were adapted for this study. First, the maximal range for <sup>90</sup>Y betas in tissue is 1.2 cm, which is in the same order of magnitude as the resolution of <sup>90</sup>Y PET, thus it was assumed the total energy is deposited within the voxel of origin<sup>17</sup>. Second, that <sup>90</sup>Y distributes uniformly in case of lung shunting, and third, lung density was the same for all patients.

### **<sup>90</sup>Y PET-based lung shunt fraction**

Since planar based  $LSF_{MAA}$  is a poor predictor for the actual lung shunting, in this work lung shunt fraction measured using <sup>90</sup>Y PET/CT ( $LSF_{Y-90}$ ) was used as metric to evaluate differences in biology.

To assess differences among tumor type,  $LSF_{Y-90}$  was computed.  $LSF_{Y-90}$  was defined as the ratio between the activity in the lungs and the total activity administered, as follow:

$$LSF_{Y-90} = \frac{\text{Mean Activity Concentration}_{LUNGS} \left[ \frac{Bq}{mL} \right] \times \text{Lungs volume [mL]}}{\text{Activity}_{prescribed} [Bq]} \times 100\%$$

As for the  $LMD_{Y-90}$ , mean activity concentration in the lungs was computed as the mean of the voxel value [Bq/mL] within both lungs mask. Lungs volume was assumed to be the same among all subjects, considering a lung mass of 1 kg and a lung density value of  $2.6e^{-4}$  [kg/mL], previously assumed.

### **Statistical analysis**

Statistical variables under investigation to characterize radiation pneumonitis were  $LMD_{MAA}$  and  $LMD_{Y-90}$ . When assessing the eventual difference among tumor types or, in case of HCC patients, between the presence or not of portal hypertension and thrombus,  $LSF_{Y-90}$  was considered, to take into account the different activity delivered. The normality of their distribution was assessed visually and by mean of QQ plot. If variables were not normally distributed, non-parametric test were used for further analysis.

Mann–Whitney U test with alpha significance level equal to 0.05 was used in case of HCC patients to assess whether the occurrence of thrombus or portal hypertension caused statistically significant left lung mean dose.

Kruskal-Wallis H-test with alpha significance level of 0.05 was used to determine whether statistical difference was found between different tumor types.

## **RESULTS**

### **Patients' population**

Patients and treatments characteristics are summarized in TABLE I. The institutional review board approved this study and waived the need for informed consent for this retrospective study. There were 170 men and 102 women for a total of 317 <sup>90</sup>Y radioembolization procedures (mean procedures per patient 1.17 range 1-5). Most of the patients were treated for liver metastases of various origins, while 25% had HCC. Glass microspheres were used for 200 treatments while the remaining 117 procedures were performed with resin microspheres. Median administered activity per procedure was 2278 MBq (range: 277 - 9636) and 1877 MBq (516 – 3245) for glass and resin microspheres respectively. Median volume within the PET field-of-view was 1713 cc (392 – 7851) and 733 cc (80-3792) for both lungs and left lung, respectively.

### **Data analysis**

Median LMD<sub>MAA</sub> was 3.5Gy (range: 0.2 – 89.0). For 14 patients planar LMD<sub>MAA</sub> was greater than 30Gy, above which <sup>90</sup>Y radioembolization is contraindicated<sup>18</sup>. Nonetheless, after clinical considerations by the treating physicians, these patients underwent <sup>90</sup>Y radioembolization treatment.

Median post-treatment LMD<sub>Y-90</sub> was 1.0Gy (range 0.0 – 22.1), with three cases above 12Gy. No cases of LMD<sub>Y-90</sub> above 30Gy were reported.

Median  $LSF_{Y-90}$  was 4.13% (range 0.27 – 39.02). Overall, according to Kruskal-Wallis H-test, no statistical significant difference was reported among tumor type ( $p$ -value = 0.1). However, pairwise comparison among tumor type returned a statistical significant difference between NET patients compared to CRC, HCC and “others” patients, with a  $p$ -value of 0.008, 0.010 and 0.022 respectively.  $P$ -values for statistical significance difference resulting from the pairwise comparison among tumor types in term of  $LSF_{Y-90}$  are reported in TABLE2. Boxplot depicting the  $LSF_{Y-90}$  per tumor type is shown in FIGURE.2.

$LMD_{Y-90}$  as function of  $LMD_{MAA}$  is reported in FIGURE.3. This suggested that radiation pneumonitis did not occur among subjects with a  $LMD_{Y-90}$  below 12Gy. Based on this empirical value and the 30Gy limit for  $LMD_{MAA}$ , the number of true negative, true positive, false negative and false positive was reported in FIGURE.3.

### **Radiation pneumonitis occurrence**

Radiation pneumonitis did not occur among all the subjects with a  $LMD_{Y-90}$  below 12Gy. Radiation pneumonitis occurred in two patients, both diagnosed with HCC and treated with glass microspheres. The first patient presented the highest  $LMD_{Y-90}$  (22.1Gy) among the subjects considered in this study. The patient had no thrombus neither portal hypertension. During the pre-treatment work-up  $LMD_{MAA}$  was 89.0Gy ( $LSF_{MAA} = 23\%$ ), SPECT/CT showed no evidence of extrahepatic depositions in the upper abdomen. Total administered activity was 7775 MBq. The second patient diagnosed had a  $LMD_{Y-90}$  of 17.7Gy, in the presence of both portal vein tumor thrombosis and portal hypertension.  $LMD_{MAA}$  was 34.1Gy ( $LSF_{MAA} = 50\%$ ), SPECT/CT showed no evidence of extrahepatic depositions in the upper abdomen. Total administered activity was 1300 MBq. Details of this case have been previously described by Alsultan *et al.*<sup>11</sup>.

Another subject, with  $LMD_{Y-90}$  of 18.4Gy ( $LMD_{MAA} = 29.1Gy$ ,  $LSF_{MAA} = 19\%$ ) died 2 months after treatment, before evaluation scan, due to progressive disease.

## DISCUSSIONS

The limit of 30Gy as maximum absorbed dose to the lungs for single radioembolization treatment was based on clinical evidence from two seminal publications<sup>4,5</sup> that have strongly influenced the guidance on lung dose limits following radioembolization. In this observational study, it has been shown that no patients with LMD<sub>Y-90</sub> below 12Gy developed any lung-dose related side effect. Out of the 14 patients who had a LMD<sub>MAA</sub> above 30Gy, two of them developed radiation pneumonitis. However, the twelve other patients with LMD<sub>MAA</sub> > 30Gy did not developed any lung-dose related side effect, remarking the limitation of using <sup>99m</sup>Tc-MAA planar scintigraphy in predicting <sup>90</sup>Y lung shunt.

Radiation pneumonitis is a rare but potentially fatal side effect of radioembolization. During the past years different works, summarized by Cremonesi *et al.*<sup>19</sup>, have been published reporting the lung-dose related side effect of <sup>90</sup>Y radioembolization, trying to provide a better insight in defining the upper dose limit to the lungs. However, although they all used the same approach to compute the lung dose, namely the <sup>99m</sup>Tc-MAA scintigraphy acquired prior to the <sup>90</sup>Y treatment and then multiplying the resulting LSF<sub>MAA</sub> by the administered activity to estimate the LMD, different values for the lung dose above which radiation pneumonitis occurred were found (ranging between 10Gy and 56Gy). In line with the 12 false positive reported in this study (see FIGURE.3), Salem *et al.*<sup>20</sup>, reported of 58 patients treated with cumulative and/or single treatment lung doses based on LSF<sub>MAA</sub> derived calculations exceeding 30Gy who did not develop any radiation pneumonitis or lung toxicities. These findings further underline how <sup>99m</sup>Tc particle overestimates the actual lung shunt. On the contrary, Leung *et al.*<sup>4</sup> already reported radiation pneumonitis occurrence in three patients with a predicted lung mean dose lower than 30Gy. It is important to note, though, that the absorbed doses taken from the literature were derived without including the attenuation correction and thus should be rescaled by an average factor of 0.6<sup>21</sup>. For this reason, a straight comparison with the results presented in this study is difficult. In addition, in this study, LMD<sub>Y-90</sub> was computed on the post treatment <sup>90</sup>Y PET and considering only the left lung as representative for the lungs volume. In this study, the same difficulties were found in determining a unique threshold for the <sup>99m</sup>Tc-MAA based LMD estimate values

to avoid radiation pneumonitis, confirming an issue well documented in literature. As an example, in a multicenter study, Braat *et al.*<sup>20</sup> reported a patient with  $LSF_{MAA}$  of 3% who developed radiation pneumonitis, while another patient with the highest  $LSF_{MAA}$ , equal to 33%, did not develop a radiation pneumonitis. These contradictory findings in literature underline the limits of planar  $^{99m}Tc$ -MAA lung shunt fraction, and consequently lung dose estimate, as predictive particle for assessing  $^{90}Y$  distribution<sup>9</sup>, stressing the need for a more reliable and robust method or particle. In the recent years, some alternatives to  $^{99m}Tc$ -MAA were suggested. Kunnen *et al.*<sup>22</sup> demonstrated, in a phantom study, that bremsstrahlung SPECT/CT, reconstructed with a Monte Carlo algorithm, can estimate the lung shunt fraction for a  $^{90}Y$  pretreatment procedure using a theoretically safe  $^{90}Y$  activity as low as 70 MBq.  $^{166}Ho$  scout microspheres (250 MBq, QuiremScout®), already used as scout particles prior to  $^{166}Ho$  radioembolization, were proposed as surrogate of  $^{90}Y$  to determine patients' eligibility, thanks to its imaging possibility<sup>23</sup>.

Both patients who developed radiation pneumonitis in this study had HCC. Both cirrhosis and HCC have been associated with increased arterio-venous shunting into the lungs, potentially causing increased lung doses<sup>24</sup>. However, significant differences were observed in  $LSF_{Y-90}$  only for HCC patients when compared to NET diagnosed subjects (FIGURE.2). In the subgroup of HCC patients only, the presence of either a thrombus or portal hypertension did not play a statistically significant role in  $LSF_{Y-90}$ , suggesting that these variables might be negligible when assessing the lung-dose related side effect of  $^{90}Y$ . Conversely, Ward *et al.*<sup>25</sup>, who reviewed 409 patients, reported a low, but significant, correlation between increased hepatopulmonary shunt fraction, measured using planar  $^{99m}Tc$ -MAA, and HCC, hepatic vein tumor thrombus and portal vein tumor thrombus. Several limitations apply to this study, apart from its retrospective and single-center nature. Considering the planar  $^{99m}Tc$  based  $LMD_{MAA}$  computation, the main limitation is the use of a surrogate model using MAA particle as an approximation to  $^{90}Y$  microsphere distribution. In addition, lungs and liver were delineated on planar scintigraphy without anatomical reference and assuming a fixed lung mass of 1 kg. This means that female patients, who have a smaller organ mass<sup>26,27</sup>, with the same lung shunt as male patients may have received a larger lung radiation dose for the same treatment

activity. As for the  $^{90}\text{Y}$  PET based  $\text{LMD}_{\text{Y-90}}$  computation, a constant value for the lung density was used. However, as reported by Kappadath *et al.*<sup>28</sup>, this might be a limiting factor in an accurate estimate of the  $\text{LMD}_{\text{Y-90}}$ . Although this study relied on the assumption of lung homogeneity, given the incomplete lungs within the PET field of view for some dataset, the distribution of microspheres in vivo is heterogeneous<sup>17</sup>. The gravitational dependence of alveolar and vascular pressures within the lung cause preferential distribution of blood flow and, in parallel, microspheres to the bases of the lung<sup>29</sup>. In addition, microsphere irradiation is microscopically nonuniform<sup>30</sup>. However, in case of radiation pneumonitis occurrence, the assumption of uniform distribution in the lung was visually confirmed by the contrast enhanced CT acquired during the follow-up. Regardless, these limitations are a reflection of the current protocols and the treatment of patients. Moreover, radiation pneumonitis is a rare side effect of radioembolization, with just two cases over 317 procedures in this study, number of events is too limited for any realistic statistical analysis.

Despite the aforementioned limitations, a better predictive particle and a new lung dose limit are essential to improve the current general patient selection avoiding unjustified patient exclusion. Given the proven value of post-treatment  $^{90}\text{Y}$  PET/CT<sup>20</sup>, more insight should be gained in the real lung dose delivered after the treatment, compared to the predicted one.

## **CONCLUSION**

This observational study showed that radiation pneumonitis did not occur among subjects with left mean lung dose below 12Gy, defined on post treatment  $^{90}\text{Y}$ -PET/CT.  $^{99\text{m}}\text{Tc}$ -MAA-based planar lung dose estimate cut-off of >30Gy is capricious and, once encountered in pre-treatment imaging, should be evaluated with caution, to prevent unjustified treatment exclusion.

## **DISCLOSURE**

MS is employed by the UMC Utrecht under a collaborative grant of the Dutch Research Council (NWO) between UMC Utrecht and Quirem Medical BV. RvR and HWAMdJ have acted as a consultant for BTG/Boston Scientific. AJATB has acted as a consultant for BTG/Boston Scientific and Terumo. MGEHL has acted as a consultant for BTG/Boston Scientific and Terumo, and receives research support from BTG/Boston Scientific and Quirem Medical BV. The department of Radiology and Nuclear Medicine of the UMC Utrecht receives royalties from Quirem Medical BV. No other potential conflicts of interest relevant to this article exist.

## **ACKNOWLEDGMENT**

We thank IT-support, in particular Marloes van Ijzendoorn, for their help and support in providing anonymized data for this study. We express gratitude to Sander Ebbers, who helped with the statistical analysis presented in this study.

## **KEY POINTS**

**Question:** What is the lung mean dose value below which radiation pneumonitis did not occur after  $^{90}\text{Y}$ -radioembolization?

**Pertinent Findings:** This retrospective cohort study showed that all the subjects with a lung mean dose below 12Gy, measured on post-treatment  $^{90}\text{Y}$  PET/CT, did not develop radiation pneumonitis.

**Implications for patient care:** Our findings suggest reconsidering the currently clinically used upper limit for lung mean dose of 30Gy.

## REFERENCE

1. Braat AJAT, Smits MLJ, Braat MNGJA, et al. 90Y hepatic radioembolization: An update on current practice and recent developments. *J Nucl Med.* 2015;56(7):1079-1087.  
doi:10.2967/jnumed.115.157446
2. Salem R, Thurston KG. Radioembolization with 90yttrium microspheres: A state-of-the-art brachytherapy treatment for primary and secondary liver malignancies - Part 1: Technical and methodologic considerations. *J Vasc Interv Radiol.* 2006;17(8):1251-1278.  
doi:10.1097/01.RVI.0000233785.75257.9A
3. Peterson JL, Vallow LA, Johnson DW, et al. Complications after 90Y microsphere radioembolization for unresectable hepatic tumors: An evaluation of 112 patients. *Brachytherapy.* 2013;12(6):573-579. doi:10.1016/j.brachy.2013.05.008
4. Leung TWT, Lau WY, Ho SKW, et al. Radiation pneumonitis after selective internal radiation treatment with intraarterial 90Yttrium-microspheres for inoperable hepatic tumors. *Int J Radiat Oncol Biol Phys.* 1995;33(4):919-924. doi:10.1016/0360-3016(95)00039-3
5. Ho S, Lau WY, Leung TWT, Chan M, Johnson PJ, Li AKC. Clinical evaluation of the partition model for estimating radiation doses from yttrium-90 microspheres in the treatment of hepatic cancer. *Eur J Nucl Med.* 1997;24(3):293-298. doi:10.1007/s002590050055
6. Kappadath SC, Lopez BP, Salem R, Lam MGEH. Reassessment of the lung dose limits for radioembolization. *Nucl Med Commun.* 2021;42(10):1064-1075.  
doi:10.1097/mnm.0000000000001439
7. Lopez B, Mahvash A, Lam MGEH, Kappadath SC. Calculation of lung mean dose and quantification of error for 90Y-microsphere radioembolization using 99mTc-MAA SPECT/CT and diagnostic chest CT. *Med Phys.* 2019;46(9):3929-3940. doi:10.1002/mp.13575

8. Elschot M, Nijssen JFW, Lam MGEH, et al.  $^{99m}\text{Tc}$ -MAA overestimates the absorbed dose to the lungs in radioembolization: a quantitative evaluation in patients treated with  $^{166}\text{Ho}$ -microspheres. *Eur J Nucl Med Mol Imaging*. 2014;41(10):1965-1975. doi:10.1007/s00259-014-2784-9
9. Wondergem M, Smits MLJ, Elschot M, et al.  $^{99m}\text{Tc}$ -macroaggregated albumin poorly predicts the intrahepatic distribution of  $^{90}\text{Y}$  resin microspheres in hepatic radioembolization. *J Nucl Med*. 2013;54(8):1294-1301. doi:10.2967/jnumed.112.117614
10. Alsultan AA, Smits MLJ, Barentsz MW, Braat AJAT, Lam MGEH. The value of yttrium-90 PET/CT after hepatic radioembolization: a pictorial essay. *Clin Transl Imaging*. 2019;7(4):303-312. doi:10.1007/s40336-019-00335-2
11. D'Arienzo M, Pimpinella M, Capogni M, et al. Phantom validation of quantitative Y-90 PET/CT-based dosimetry in liver radioembolization. *EJNMMI Res*. 2017;7(1):94. doi:10.1186/s13550-017-0341-9
12. Kunnen B, Beijst C, Lam MGEH, Viergever MA, de Jong HWAM. Comparison of the Biograph Vision and Biograph mCT for quantitative  $^{90}\text{Y}$  PET/CT imaging for radioembolisation. *EJNMMI Phys*. 2020;7(1). doi:10.1186/s40658-020-0283-6
13. Dittmann H, Kopp D, Kupferschlaeger J, et al. A prospective study of quantitative spect/CT for evaluation of lung shunt fraction before SIRT of liver tumors. *J Nucl Med*. 2018;59(9):1366-1372. doi:10.2967/jnumed.117.205203
14. Hofmanninger J, Prayer F, Pan J, Röhrich S, Prosch H, Langs G. Automatic lung segmentation in routine imaging is primarily a data diversity problem, not a methodology problem. *Eur Radiol Exp*. 2020;4(1). doi:10.1186/s41747-020-00173-2
15. Rhodes, Christopher G., Wollmer, Per, Fazio, Ferruccio, Jones T. Quantitative measurement of regional extravascular lung density using positron emission and transmission tomography. Title. *J*

*Comput Assist Tomogr.* 1982;5(6):783-791. doi:10.1097/00004728-198112000-00001

16. Pasciak AS, Bourgeois AC, Bradley YC. A comparison of techniques for <sup>90</sup>Y PET/CT image-based dosimetry following radioembolization with resin microspheres. *Front Oncol.* 2014;4 MAY(May):1-11. doi:10.3389/fonc.2014.00121
17. Bastiaannet R, Kappadath SC, Kunnen B, Braat AJAT, Lam MGEH, de Jong HWAM. The physics of radioembolization. *EJNMMI Phys.* 2018;5(1):22. doi:10.1186/s40658-018-0221-z
18. Levillain H, Bagni O, Deroose CM, et al. International recommendations for personalised selective internal radiation therapy of primary and metastatic liver diseases with yttrium-90 resin microspheres. *Eur J Nucl Med Mol Imaging.* 2021;48(5):1570-1584. doi:10.1007/s00259-020-05163-5
19. Cremonesi M, Chiesa C, Strigari L, et al. Radioembolization of Hepatic Lesions from a Radiobiology and Dosimetric Perspective. *Front Oncol.* 2014;4(August):210. doi:10.3389/fonc.2014.00210
20. Salem R, Parikh P, Atassi B, et al. Incidence of radiation pneumonitis after hepatic intra-arterial radiotherapy with yttrium-90 microspheres assuming uniform lung distribution. *Am J Clin Oncol Cancer Clin Trials.* 2008;31(5):431-438. doi:10.1097/COC.0b013e318168ef65
21. Chiesa C., Maccauro M., Romito R., Spreafico C., Pellizzari S., Negri A., Sposito C., Morosi C., Civelli E., Lanocita R., Camerini T., Bampo C., Bhoori S., Seregini E., Marchianò A., Mazzaferro V. BE. Need, feasibility and convenience of dosimetric treatment planning in liver selective internal radiation therapy with <sup>90</sup>Y microspheres: the experience of the National Tumor Institute of Milan. *Q J Nucl Med Mol imaging.* 2011;55(2):168-197. The Quarterly Journal of Nuclear Medicine and Molecular imaging.
22. Kunnen B, van der Velden S, Bastiaannet R, Lam MGEH, Viergever MA, de Jong HWAM.

Radioembolization lung shunt estimation based on a 90Y pretreatment procedure: A phantom study. *Med Phys*. 2018;45(10):4744-4753. doi:10.1002/mp.13168

23. Prince JF, van Rooij R, Bol GH, de Jong HWAM, van den Bosch MAAJ, Lam MGEH. Safety of a Scout Dose Preceding Hepatic Radioembolization with 166Ho Microspheres. *J Nucl Med*. 2015;56(6):817-823. doi:10.2967/jnumed.115.155564
24. Kallini JR, Gabr A, Salem R, Lewandowski RJ. Transarterial Radioembolization with Yttrium-90 for the Treatment of Hepatocellular Carcinoma. *Adv Ther*. 2016;33(5):699-714. doi:10.1007/s12325-016-0324-7
25. Ward TJ, Tamrazi A, Lam MGEH, et al. Management of high hepatopulmonary shunting in patients undergoing hepatic radioembolization. *J Vasc Interv Radiol*. 2015;26(12):1751-1760. doi:10.1016/j.jvir.2015.08.027
26. Molina DK, DiMaio VJM. Normal organ weights in women: Part II - The Brain, Lungs, Liver, Spleen, and Kidneys. *Am J Forensic Med Pathol*. 2015;36(3):182-187. doi:10.1097/PAF.0000000000000175
27. Molina DK, Dimaio VJM. Normal organ weights in men: Part II-the brain, lungs, liver, spleen, and kidneys. *Am J Forensic Med Pathol*. 2012;33(4):368-372. doi:10.1097/PAF.0b013e31823d29ad
28. Cheenu Kappadath S, Lopez BP, Salem R, Lam MG. Lung Shunt and Lung Dose Calculation Methods for Radioembolization Treatment Planning. *Q J Nucl Med Mol Imaging*. 2021;65(1):32-42. doi:10.23736/S1824-4785.20.03287-2
29. Armstrong J, Raben A, Zelefsky M, et al. Promising survival with three-dimensional conformal radiation therapy for non-small cell lung cancer. *Radiother Oncol*. 1997;44(1):17-22. doi:10.1016/S0167-8140(97)01907-5
30. Giammarile F, Bodei L, Chiesa C, et al. EANM procedure guideline for the treatment of liver

cancer and liver metastases with intra-arterial radioactive compounds. *Eur J Nucl Med Mol Imaging*. 2011;38(7):1393-1406. doi:10.1007/s00259-011-1812-2

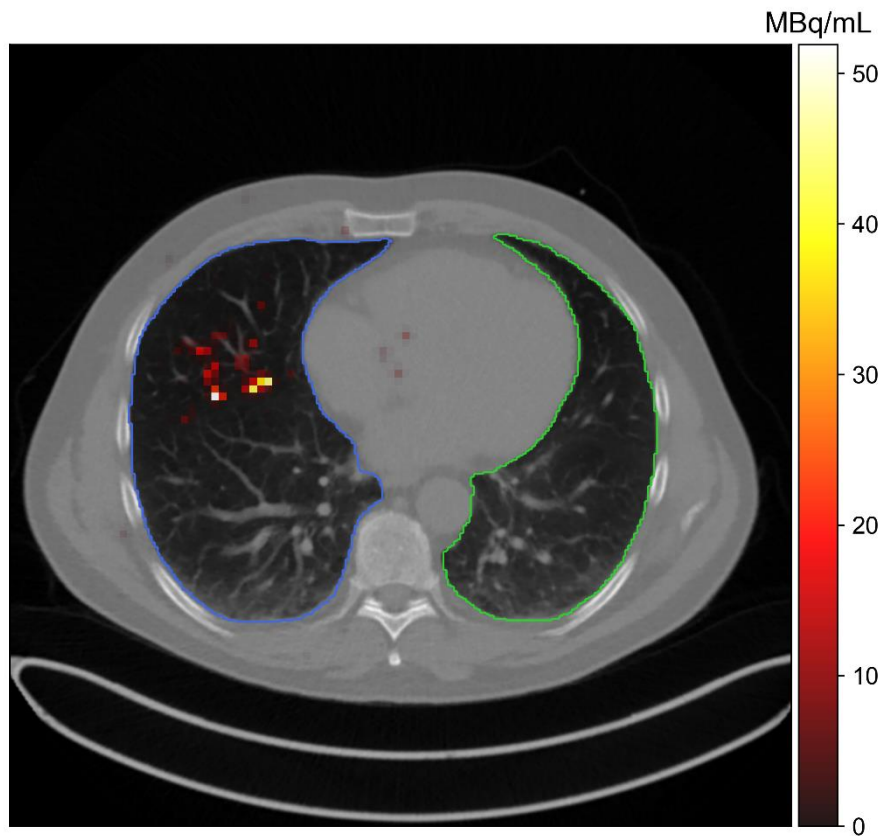


FIGURE.1

Post-treatment  $^{90}\text{Y}$  PET/CT scan of a 47 years old male patient diagnosed with CRC. Mean dose to the lungs considering both lobes was 61Gy. The  $^{90}\text{Y}$  PET image shows activity in the right lung (blue contour), due to liver motion in the cranial-caudal direction and a rim field-of-view artefact, and leading to a lung mean dose to right lung of 100Gy, which was the main contributor to the lung mean dose. Left lung mean dose (computed within the green contour) was 3Gy.

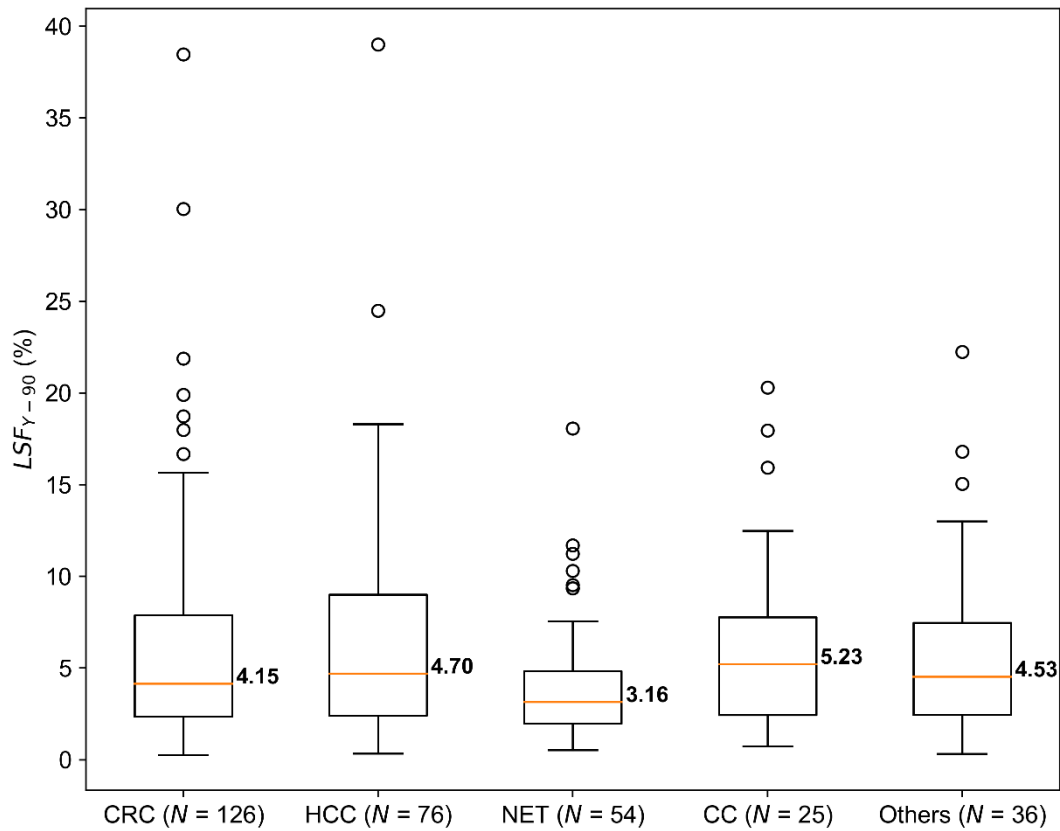


FIGURE.2

Boxplots depicting the  $^{90}\text{Y}$  PET based lung shunt fraction ( $\text{LSF}_{\text{Y-90}}$ ), together with the corresponding median value, divided by tumor type. Statistically significant difference was reported between NET and CRC patients ( $p\text{-value} = 0.008$ ), between NET and HCC patients ( $p\text{-value} 0.010$ ), and between NET and patients in the group “others” ( $p\text{-value}$  of 0.022). Acronyms used for the tumor type are CRC (colorectal cancer), HCC (hepatocellular carcinoma), NET (neuroendocrine tumor) and CC (cholangiocellular carcinoma).

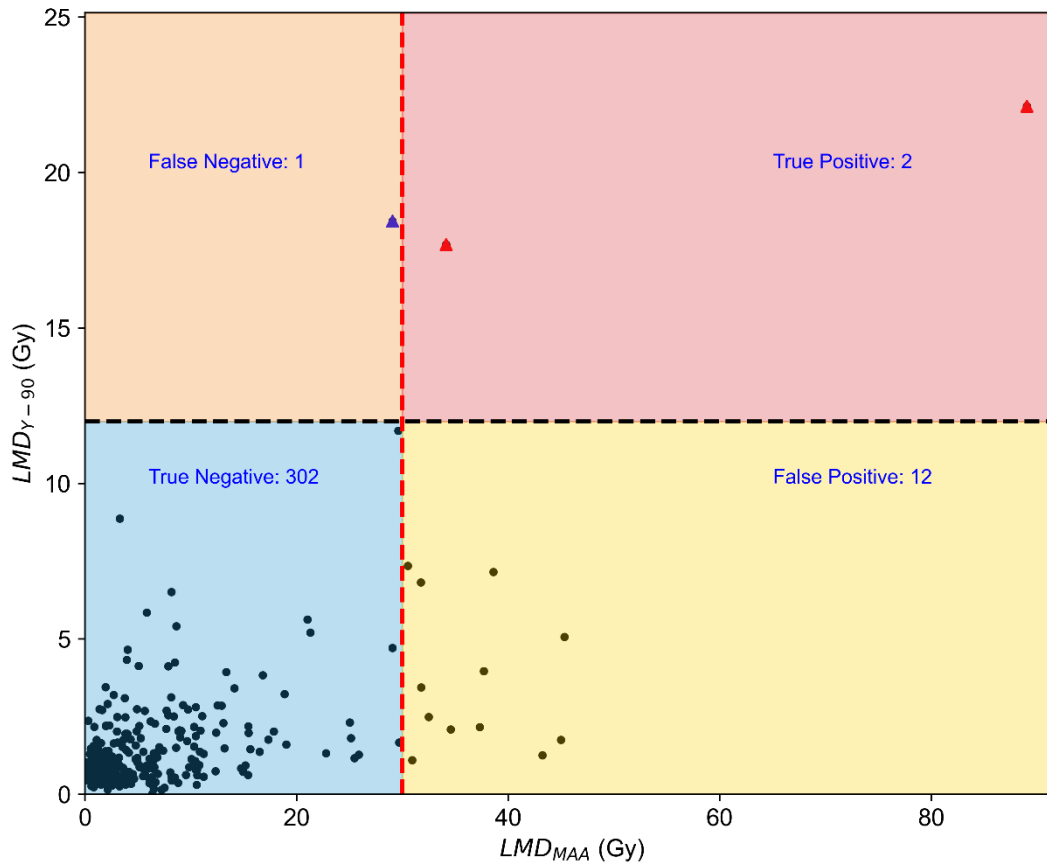


FIGURE.3

Distribution of the  $^{90}\text{Y}$  PET based left lung mean dose ( $LMD_{Y-90}$ ) as function of the corresponding planar  $^{99m}\text{Tc}$ -MAA based lung dose prediction ( $LMD_{MAA}$ ). Based on the limit of 30Gy for the estimate radiation absorbed dose to the lungs during the pre-treatment phase and value of 12Gy for  $LMD_{Y-90}$ , below which no radiation pneumonitis cases were reported, subjects were divided in four quadrants. (I) TP, the true positive quadrant (red), (II) FP, the false positive quadrant (yellow); (III) TN, the true negative quadrant (blue); and (IV) FN, the false negative quadrant (orange). According to the chosen limits, 12 false positives were detected. The true positive (red triangles) correspond to the two patients who developed radiation pneumonitis, while the false negative (blue triangle) correspond to a patient who died due to progressive disease before follow-up.

TABLE.1. Baseline and treatment characteristics

<b>Characteristic</b>	<b>N (%) or median (range)</b>
Patients	272
Procedures	317
<b>Sex</b>	
Male (%)	170 (62.5)
Female (%)	102 (37.5)
Mean Age (range)	64.56 (17 - 90)
<b>Spheres Type</b>	
Glass (%)	200 (63)
Resin (%)	117 (37)
<b>Median Administered Activity (MBq) (range)</b>	
Glass	2278 (277 – 9636)
Resin	1877 (516 – 3245)
Mean number of Y90 sessions (range)	1.17 (1 – 5 )
<b>Tumor Types N (%)</b>	
CRC (colorectal cancer)	104 (38%)
HCC (hepatocellular carcinoma)	68 (25%)
NET (neuroendocrine tumor)	45 (16%)
CC (cholangiocellular carcinoma)	21 (8%)
Others	34 (13%)
<b>Thrombus</b>	
Segmental right portal vein	9
Lobar left portal vein	4
Segmental R portal vein+lobar L portal vein	1
TT main portal vein	2
TT right hepatic vein	1
Portal Hypertension	33
<b>Planar MAA LSF (%)</b>	
Mean (range)	5.73 (0.49 – 50.44)
Median (IQR)	3. 87 (4.60)
Number of cases > 20%	11
<b><sup>90</sup>Y LSF (%)</b>	
Mean (range)	5.90 (0.27 – 39.02)
Median (IQR)	4.13 (5.28)
Number of cases > 20%	7
<b><sup>99m</sup>Tc based lung mean dose prediction (Gy)</b>	
Mean (range)	6.93 (0.17 – 89.03)
Median (IQR)	3. 52 (6.48)
Number of cases > 30Gy	14
<b><sup>90</sup>Y PET based left lung dose (Gy)</b>	
Mean (range)	1.59 (0.02 – 22.14)
Median (IQR)	0.95 (1.16)
Number of cases > 12Gy	3
<b>Total Lung volume (cc)</b>	
Median (range)	1713 (392 – 7851)
<b>Left Lung volume (cc)</b>	
Median (range)	733 (80 - 3792)

TABLE.2. Matrix of the statistical significance of the differences between the tumor types in terms of LSF<sub>Y-90</sub>.

<sup>90</sup>. P-values in bold are statistically significant (<0.05).

	LSF <sub>Y-90</sub>				
	<i>CC</i>	<i>CRC</i>	<i>HCC</i>	<i>NET</i>	<i>Others</i>
<i>CC</i>	-	0.5	0.5	0.06	0.5
<i>CRC</i>		-	0.4	<b>0.008</b>	0.5
<i>HCC</i>			-	<b>0.01</b>	0.4
<i>NET</i>				-	<b>0.02</b>
<i>Others</i>					-